Chin. J. Mech. Eng. (2017) 30:217–221
DOI 10.1007/s10033-017-0045-0

RESEARCH HIGHLIGHT

New Family of RPR-Equivalent Parallel Mechanisms: Design and Application

Qinchuan LI[1] · Lingmin XU[1] · Qiaohong CHEN[2] · Wei YE[1]

Published online: 23 March 2017

Parallel mechanisms(PMs) have been used as skeletons or end-effectors in various advanced manufacturing equipment. Compared with their serial counterparts, PMs offer high rigidity, good dynamic response, and large payload capability. Three-degrees-of-freedom(DOFs) parallel mechanisms with two rotational and one translational(2R1T) motion are particularly useful, such as Z3 head [1], A3 head [2], Tricept [3], and Exechon [4].

Fig 1(a) shows a three-DOF RPR serial kinematic chain, whose end-effector can perform two rotations and one translation. The two axes of rotation do not intersect and remain perpendicular. An RPR-equivalent PM can implement the two rotations and one translation of an RPR serial chain; see Figs. 1(b)–(d). Numerous new architectures for RPR-equivalent PMs have been proposed [5]. The RPR-equivalent PMs are suitable for multiple manipulations along a curved surface when high rigidity, accuracy and dexterity are required, such as for five-axis machining [6], aircraft wing assembly [7], and friction stir welding [8].

To the best of our knowledge, the RPR-equivalent PM is the 2R1T PM with the fewest single-DOF joints. For example, the parallel module of the Exechon robot, which is based on a 2UPR-SPR PM, has 13 single-DOF joints; the Trivaiant hybrid robot, based on a 2UPS-UP PM, has 15 single-DOF joints [9]; the Tricept hybrid robot, based on a 3UPS-UP PM, has 21 single-DOF joints; the Z3 articulated head, based on a 3-PRS PM, has 15 single-DOF joints. It is worth mentioning that better accuracy and stiffness can be achieved when there are fewer single-DOF joints, because the kinematic joint is a weak point that is the main cause of deformation and clearance issues.

The most important topics in improving the performance of PMs concern their stiffness and dynamic response. An efficient approach is to use fixed linear actuators, which require heavy powerful servomotors and reduced movable mass. LIU, et al [10], presented a family of 1R2T PMs with high rotational capability, some of which can be fully maneuvered by fixed linear actuators. Based on Grassmann line geometry and the atlas method, several 4-DOF PMs with fixed linear actuators have been synthesized [11], and the inverse dynamics of a translational PM with three fixed linear actuators have been studied [12]. However, there are few RPR-equivalent PMs with fixed linear actuators.

To fill this gap, this paper presents a new family of RPR-equivalent PMs that can be fully or partly actuated with fixed linear actuators [13]. As listed in Table 1, the common feature of these PMs is that there is at least one ${}^{u}P^{uv}U^{v}R$ limb or ${}^{u}PS^{v}R$ limb(superscripts u and v denote the axial directions of related joints) that can be actuated by fixed linear actuators.

There are four important geometrical conditions in these PMs.

(1) If there are two ${}^{u}P^{uv}U^{v}R$ limbs in a PM, the first rotational axes of the two U joints should be coincident.
(2) If there are two ${}^{u}\underline{RP}^{uv}U$, two ${}^{u}\underline{RR}^{uv}U$, or two ${}^{u}\underline{PR}^{uv}U$ limbs in a PM, the second rotational axes of the two U joints should be coincident.
(3) If there are two ${}^{u}PS^{v}R$ limbs in a PM, the line passing through the centers of the two S joints should be parallel to vector $\boldsymbol{u}$.

✉ Qinchuan LI
lqchuan@zstu.edu.cn

1 Faculty of Mechanical Engineering and Automation, Zhejiang Sci-Tech University, Hangzhou 310018, China

2 School of Information, Zhejiang Sci-Tech University, Hangzhou 310018, China

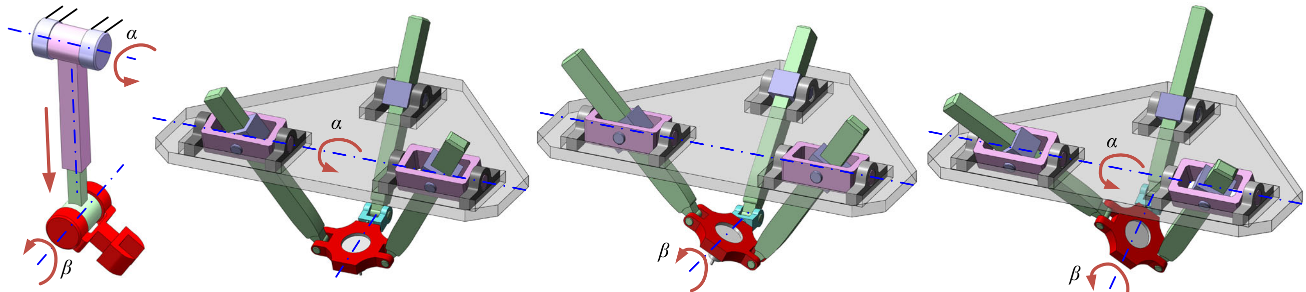

(a) RPR serial kinematic chain **(b)** Rotation around the fixed axis **(c)** Rotation around the moving axis **(d)** Rotations around two axes

Fig. 1 RPR serial kinematic chain and its equivalent PM

Table 1 New RPR-equivalent PMs

Categories	PMs
4-4-4 category	$2\text{-}{}^{u}P^{uv}U^{v}R/\underline{{}^{u}RP}^{uv}U$, $2\text{-}\underline{{}^{u}RP}^{uv}U/{}^{u}P^{uv}U^{v}R$ $2\text{-}{}^{u}P^{uv}U^{v}R/\underline{{}^{u}RR}^{uv}U$, $2\text{-}\underline{{}^{u}RR}^{uv}U/{}^{u}P^{uv}U^{v}R$ $2\text{-}{}^{u}P^{uv}U^{v}R/\underline{{}^{u}PR}^{uv}U$, $2\text{-}\underline{{}^{u}PR}^{uv}U/{}^{u}P^{uv}U^{v}R$
4-4-5 category	$2\text{-}{}^{u}P^{uv}U^{v}R/\underline{{}^{u}RP}S$, $2\text{-}\underline{{}^{u}RP}^{uv}U/{}^{u}PS^{v}R$ $2\text{-}{}^{u}P^{uv}U^{v}R/\underline{{}^{u}RR}S$, $2\text{-}\underline{{}^{u}RR}^{uv}U/{}^{u}PS^{v}R$ $2\text{-}{}^{u}P^{uv}U^{v}R/\underline{{}^{u}PR}S$, $2\text{-}\underline{{}^{u}PR}^{uv}U/{}^{u}PS^{v}R$
5-5-4 category	$2\text{-}{}^{u}PS^{v}R/\underline{{}^{u}RP}^{uv}U$, $2\text{-}\underline{{}^{u}RP}S/{}^{u}P^{uv}U^{v}R$ $2\text{-}{}^{u}PS^{v}R/\underline{{}^{u}RR}^{uv}U$, $2\text{-}\underline{{}^{u}RR}S/{}^{u}P^{uv}U^{v}R$ $2\text{-}{}^{u}PS^{v}R/\underline{{}^{u}PR}^{uv}U$, $2\text{-}\underline{{}^{u}PR}S/{}^{u}P^{uv}U^{v}R$
5-5-5 category	$2\text{-}{}^{u}PS^{v}R/\underline{{}^{u}RP}S$, $2\text{-}\underline{{}^{u}RP}S/{}^{u}PS^{v}R$ $2\text{-}{}^{u}PS^{v}R/\underline{{}^{u}RR}S$, $2\text{-}\underline{{}^{u}RR}S/{}^{u}PS^{v}R$ $2\text{-}{}^{u}PS^{v}R/\underline{{}^{u}PR}S$, $2\text{-}\underline{{}^{u}PR}S/{}^{u}PS^{v}R$

Note: The underline in $\underline{{}^{u}RP}$, $\underline{{}^{u}RR}$, and $\underline{{}^{u}PR}$ denotes that they belong to the three-dimensional planar subgroup $\{\boldsymbol{G}(\boldsymbol{u})\}$, *X*-*Y*-*Z* category means the DOFs of the limbs are *X*, *Y*, and *Z*, respectively

(4) If there are two $\underline{{}^{u}RP}^{uv}S$, two $\underline{{}^{u}RR}^{uv}S$, or two $\underline{{}^{u}PR}^{uv}S$ limbs in a PM, the line passing through the centers of the two S joints should be parallel to vector $\boldsymbol{v}$.

For clarity, some of the RPR-equivalent PMs are sketched in Fig. 2. Hereafter, the axes of rotations of the PMs will be represented in the figures by dotted blue lines.

To verify the validity of the proposed designs, Lie group theory [14, 15] is adopted to conduct the DOFs analysis of the PM in Fig. 2(a). The kinematic bond of limb 1 is

$$\{\boldsymbol{L}_1\}=\{\boldsymbol{T}(\boldsymbol{u})\}\{\boldsymbol{R}(A_1,\boldsymbol{u})\}\{R(\boldsymbol{A}_1,\boldsymbol{v})\}\{R(B_1,\boldsymbol{v})\}, \tag{1}$$

where $\{\boldsymbol{T}(\boldsymbol{u})\}$ represents a translation along $\boldsymbol{u}$, $\{\boldsymbol{R}(A_1, \boldsymbol{u})\}$ represents a rotation around the axis in direction $\boldsymbol{u}$ and passing through point A_1, A_1 is the center of the universal joint in limb 1, and B_1 is the center of the revolute joint. Vectors $\boldsymbol{u}$ and $\boldsymbol{v}$ represent the directions of the related joints. It is easy to find that $\{\boldsymbol{T}(\boldsymbol{u})\}\{\boldsymbol{R}(A_1, \boldsymbol{u})\}$ constitutes a cylindrical subgroup $\{\boldsymbol{C}(A_1, \boldsymbol{u})\}$. Because of the closure of products in subgroup $\{\boldsymbol{C}(A_1, \boldsymbol{u})\}$, $\{\boldsymbol{L}_1\}$ can be rewritten as

$$\{\boldsymbol{L}_1\}=\{\boldsymbol{R}(A_1,\boldsymbol{u})\}\{\boldsymbol{T}(\boldsymbol{u})\}\{\boldsymbol{R}(A_1,\boldsymbol{v})\}\{R(\boldsymbol{B}_1,\boldsymbol{v})\}. \tag{2}$$

Vector $\boldsymbol{u}$ is perpendicular to vector $\boldsymbol{v}$, so $\{\boldsymbol{T}(\boldsymbol{u})\}\{\boldsymbol{R}(A_1, \boldsymbol{v})\}\{\boldsymbol{R}(B_1, \boldsymbol{v})\}$ can be substituted by a planar subgroup $\{\boldsymbol{G}(\boldsymbol{v})\}$, which leads to

$$\{\boldsymbol{L}_1\}=\{\boldsymbol{R}(A_1,\boldsymbol{u})\}\{\boldsymbol{G}(\boldsymbol{v})\}. \tag{3}$$

Similarly, the kinematic bond of limb 2 is identified as

$$\{\boldsymbol{L}_2\}=\{\boldsymbol{R}(A_2,\boldsymbol{u})\}\{\boldsymbol{G}(\boldsymbol{v})\}. \tag{4}$$

Because A_1A_2 passes through point O and is parallel to axis $\boldsymbol{u}$, $\{\boldsymbol{R}(A_1, \boldsymbol{u})\} = \{\boldsymbol{R}(A_2, \boldsymbol{u})\} = \{\boldsymbol{R}(O, \boldsymbol{u})\}$. The intersection of $\{\boldsymbol{L}_1\}$ and $\{\boldsymbol{L}_2\}$ can be given by

$$\begin{aligned}\{\boldsymbol{L}_1\}\cap\{\boldsymbol{L}_2\} &= \{\boldsymbol{R}(A_1,\boldsymbol{u})\}\{\boldsymbol{G}(\boldsymbol{v})\}\cap\{\boldsymbol{R}(A_2,\boldsymbol{u})\}\{\boldsymbol{G}(\boldsymbol{v})\}\\ &= \{\boldsymbol{R}(O,\boldsymbol{u})\}\{\boldsymbol{G}(\boldsymbol{v})\}.\end{aligned} \tag{5}$$

The kinematic bond of limb 3 is

$$\{\boldsymbol{L}_3\}=\{\boldsymbol{R}(A_3,\boldsymbol{u})\}\{\boldsymbol{T}(\boldsymbol{x})\}\{\boldsymbol{R}(B_3,\boldsymbol{u})\}\{\boldsymbol{R}(B_3,\boldsymbol{v})\}, \tag{6}$$

where A_3 is the center of the revolute joint in limb 3, B_3 is the center of the universal joint, vector $\boldsymbol{x}$ denotes the direction of the prismatic joint, and $\boldsymbol{x}\perp\boldsymbol{u}$. Thus, $\{L_3\}$ can be rewritten as

$$\{\boldsymbol{L}_3\}=\{\boldsymbol{G}(\boldsymbol{u})\}\{\boldsymbol{R}(B_3,\boldsymbol{v})\}. \tag{7}$$

The motion set of the moving platform is as follows:

$$\begin{aligned}\{\boldsymbol{L}_1\}\cap\{\boldsymbol{L}_2\}\cap\{\boldsymbol{L}_3\} &= \{\boldsymbol{R}(O,\boldsymbol{u})\}\{\boldsymbol{G}(\boldsymbol{v})\}\cap\{\boldsymbol{G}(\boldsymbol{u})\}\{\boldsymbol{R}(B_3,\boldsymbol{v})\}\\ &= \{\boldsymbol{R}(O,\boldsymbol{u})\}\{\boldsymbol{T}(\boldsymbol{w})\}\{\boldsymbol{R}(B_3,\boldsymbol{v})\},\end{aligned} \tag{8}$$

where $\boldsymbol{w}$ is a vector that is perpendicular to $\boldsymbol{u}$ and $\boldsymbol{v}$. This equation implies that the mechanism in Fig. 2(a) is an RPR-equivalent PM. Similarly, all the mechanisms in Table 1 can be shown to be RPR-equivalent PMs.

As some of the PMs in Table 1 contain ${}^{u}PS^{v}R$ limbs, one may think that ${}^{v}PS^{u}R$-type limbs can also be used.

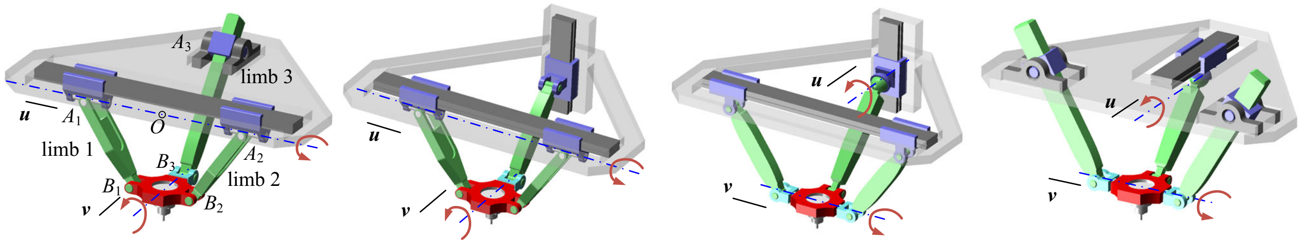

(a) $2\text{-}{}^{u}P^{uv}U^{v}R/{}^{u}\underline{RP}^{uv}U$ PM **(b)** $2\text{-}{}^{u}P^{uv}U^{v}R/{}^{u}\underline{PR}^{uv}U$ PM **(c)** $2\text{-}{}^{u}\underline{PR}^{uv}U/{}^{u}PS^{v}R$ PM **(d)** $2\text{-}{}^{u}\underline{RP}^{uv}U/{}^{u}PS^{v}R$ PM

(e) $2\text{-}{}^{u}PS^{v}R/{}^{u}\underline{PR}^{uv}U$ PM **(f)** $2\text{-}{}^{u}PS^{v}R/{}^{u}\underline{RP}S$ PM **(g)** $2\text{-}{}^{u}\underline{RP}S/{}^{u}PS^{v}R$ PM **(h)** $2\text{-}{}^{u}PS^{v}R/{}^{u}\underline{PR}S$ PM

Fig. 2 RPR-equivalent PMs

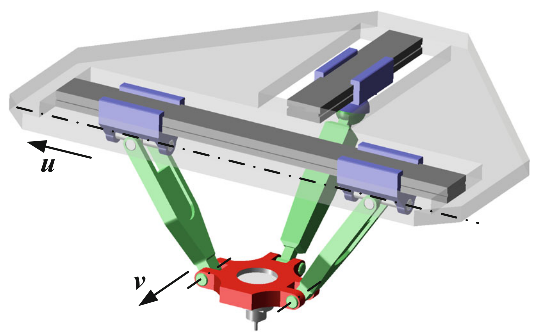

Fig. 3 Exechon-equivalent PM

However, this is not the case. For example, if two ${}^{u}P^{uv}U^{v}R$ limbs and one ${}^{v}PS^{u}R$ limb were used to connect a moving platform and a fixed base, the PM [16] would be as shown in Fig. 3. One can easily find that this has the same motion characteristic as the parallel part of the Exechon robot, but it is not an RPR-equivalent PM.

A major problem when studying PMs concerns singularities [17], which will cause side effects such as segmentation of the workspace or a decrease in stiffness. An effective way to eliminate singularities is to use redundant actuations [18, 19]. Moreover, redundant actuations can improve the force-carrying capabilities of PMs [20]. Thus, it is meaningful to design redundantly actuated RPR-equivalent PMs.

To obtain the desired structures, we adopt the method of adding a kinematic limb that contains an actuated joint to an existing RPR-equivalent PM. We do not consider 6-DOF limbs, as they can be added arbitrarily. Only lower mobility limbs that constrain some motion are concerned. For the RPR-equivalent PMs, the kinematic bond of the added limb should contain the motion set $\{\boldsymbol{R}(O, \boldsymbol{u})\}\{\boldsymbol{T}(\boldsymbol{w})\}\{\boldsymbol{R}(B_3, \boldsymbol{v})\}$. The mechanical generators of $\{\boldsymbol{R}(O, \boldsymbol{u})\}\{\boldsymbol{G}(\boldsymbol{v})\}$, $\{\boldsymbol{G}(\boldsymbol{u})\}\{\boldsymbol{R}(B_3, \boldsymbol{v})\}$, and $\{\boldsymbol{X}(\boldsymbol{u})\}\{\boldsymbol{X}(\boldsymbol{v})\}$ can be added. A vast number of limbs are usable and numerous redundantly actuated RPR-equivalent PMs can be constructed. From Eq. (5), it is clear that the ${}^{u}P^{uv}U^{v}R$ limb is the mechanical generator of $\{\boldsymbol{R}(O, \boldsymbol{u})\}\{\boldsymbol{G}(\boldsymbol{v})\}$, and one can easily find that ${}^{u}PS^{v}R$ limbs contain the bond $\{\boldsymbol{R}(O, \boldsymbol{u})\}\{\boldsymbol{G}(\boldsymbol{v})\}$. Table 2 lists the redundantly actuated RPR-equivalent PMs with four limbs; two of these are ${}^{u}P^{uv}U^{v}R$ or ${}^{u}PS^{v}R$ limbs and the left two are identical.

Table 2 Redundantly actuated RPR-equivalent PMs

Categories	PMs
4-4-4-4 category	$2\text{-}{}^{u}P^{uv}U^{v}R/2\text{-}{}^{u}\underline{RP}^{uv}U$, $2\text{-}{}^{u}P^{uv}U^{v}R/2\text{-}{}^{u}\underline{RR}^{uv}U$ $2\text{-}{}^{u}P^{uv}U^{v}R/2\text{-}{}^{u}\underline{PR}^{uv}U$
4-4-5-5 category	$2\text{-}{}^{u}P^{uv}U^{v}R/2\text{-}{}^{u}\underline{RP}S$, $2\text{-}{}^{u}\underline{RP}^{uv}U/2\text{-}{}^{u}PS^{v}R$ $2\text{-}{}^{u}P^{uv}U^{v}R/2\text{-}{}^{u}\underline{RR}S$, $2\text{-}{}^{u}\underline{RR}^{uv}U/2\text{-}{}^{u}PS^{v}R$ $2\text{-}{}^{u}P^{uv}U^{v}R/2\text{-}{}^{u}\underline{PR}S$, $2\text{-}{}^{u}\underline{PR}^{uv}U/2\text{-}{}^{u}PS^{v}R$
5-5-5-5 category	$2\text{-}{}^{u}PS^{v}R/2\text{-}{}^{u}\underline{RP}S$, $2\text{-}{}^{u}PS^{v}R/2\text{-}{}^{u}\underline{RR}S$ $2\text{-}{}^{u}PS^{v}R/2\text{-}{}^{u}\underline{PR}S$

Note: The underline in ${}^{u}\underline{RP}$, ${}^{u}\underline{RR}$, and ${}^{u}\underline{PR}$ denotes that they belong to the three dimensional planar subgroup $\{\boldsymbol{G}(\boldsymbol{u})\}$, *X-X-Y-Y* category means the DOFs of the limbs are *X* and *Y*

Note that the aforementioned four geometrical conditions for nonredundant RPR-equivalent PMs are also necessary for the redundantly actuated ones in Table 2. The $2\text{-}{}^{u}P^{uv}U^{v}R/2\text{-}{}^{u}\underline{RP}^{uv}U$ PM, $2\text{-}{}^{u}P^{uv}U^{v}R/2\text{-}{}^{u}\underline{PR}^{uv}U$ PM, $2\text{-}{}^{u}P^{uv}U^{v}R/2\text{-}{}^{u}\underline{RP}S$ PM, $2\text{-}{}^{u}P^{uv}U^{v}R/2\text{-}{}^{u}\underline{PR}S$ PM, $2\text{-}{}^{u}\underline{PR}^{uv}U/2\text{-}{}^{u}PS^{v}R$ PM, $2\text{-}{}^{u}\underline{RP}^{uv}U/2\text{-}{}^{u}PS^{v}R$ PM, $2\text{-}{}^{u}PS^{v}R/2\text{-}{}^{u}\underline{RP}S$ PM,

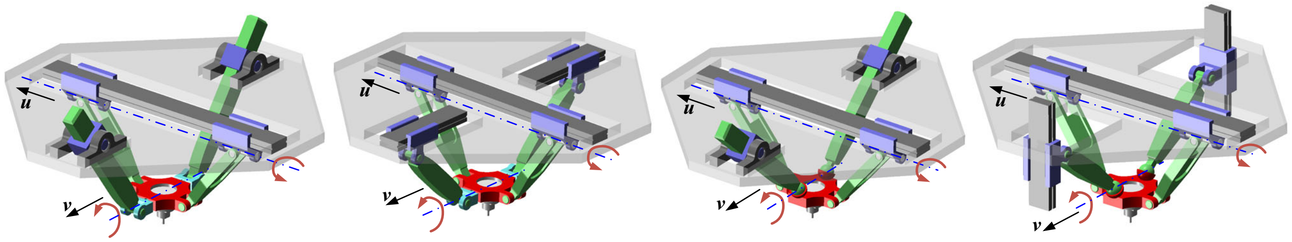

(a) $2\text{-}{}^{u}P^{uv}U^{v}R/2\text{-}{}^{u}\underline{RP}^{uv}U$ PM **(b)** $2\text{-}{}^{u}P^{uv}U^{v}R/2\text{-}{}^{u}\underline{PR}^{uv}U$ PM **(c)** $2\text{-}{}^{u}P^{uv}U^{v}R/2\text{-}{}^{u}\underline{RP}S$ PM **(d)** $2\text{-}{}^{u}P^{uv}U^{v}R/2\text{-}{}^{u}\underline{PR}S$ PM

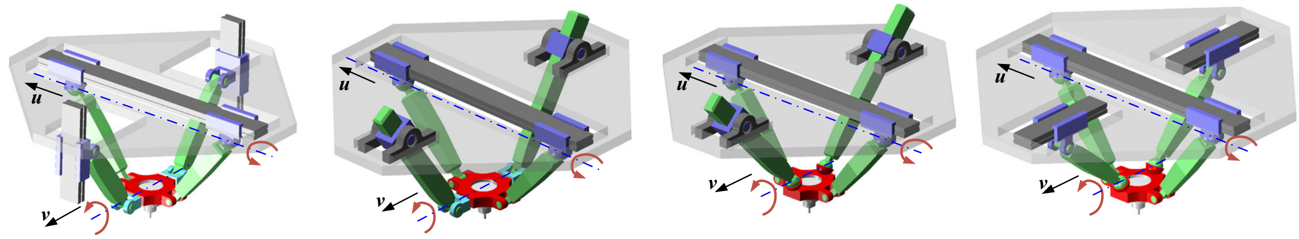

(e) $2\text{-}{}^{u}\underline{PR}^{uv}U/2\text{-}{}^{u}PS^{v}R$ PM **(f)** $2\text{-}{}^{u}\underline{RP}^{uv}U/2\text{-}{}^{u}PS^{v}R$ PM **(g)** $2\text{-}{}^{u}PS^{v}R/2\text{-}{}^{u}\underline{RP}S$ PM **(h)** $2\text{-}{}^{u}PS^{v}R/2\text{-}{}^{u}\underline{PR}S$ PM

Fig. 4 Redundantly actuated RPR-equivalent PMs

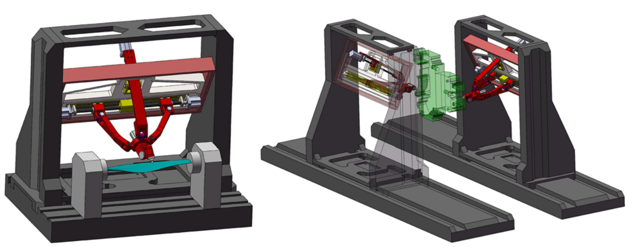

(a) Machining on a free surface **(b)** Cooperative operation

Fig. 5 Five-axis machine

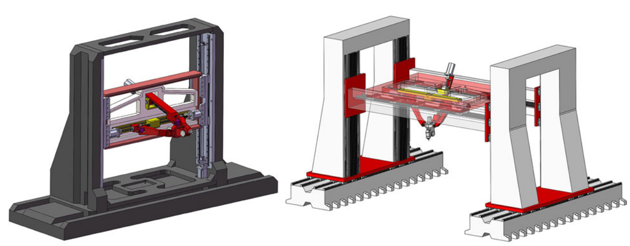

(a) A vertical machining center **(b)** A gantry moving system

Fig. 6 Machining centers

and $2\text{-}{}^{u}PS^{v}R/2\text{-}{}^{u}\underline{PR}S$ PM are sketched in Fig. 4 as examples.

The proposed RPR-equivalent PMs can be fully or partly actuated by fixed linear actuators. This is an outstanding merit that will benefit their dynamic response. The design results can be used to develop various machining centers. For example, a 2-DOF wrist can be attached to the moving platform of the $2\text{-}{}^{u}P^{uv}U^{v}R/{}^{u}\underline{RP}^{uv}U$ PM to construct the hybrid five-axis machine in Fig. 5(a). The parallel part is used to locate the platform and the serial part adjusts the orientation of the tool. Therefore, operations can be carried out on complex surfaces. If two machines are operated in coordination, as in Fig. 5(b), the efficiency can be dramatically improved. To increase the workspace and flexibility, one can install the machine on a translational gantry to form a vertical machine center or a 2-DOF gantry to form a gantry moving system, as in Fig. 6(a) and Fig. 6(b), respectively. Because of the advantages of the parallel part, good performance can be expected from these machines.

This study is the first step towards developing new high-performance parallel/hybrid kinematic machines. Future work will concentrate on the kinematic analysis, dynamics, optimal design, calibration, development of prototypes, and verification experiments.

Acknowledgements The authors would like to acknowledge the financial support of National Natural Science Foundation of China(NSFC) under Grant Nos. 51525504, 51475431, 51275479, and Zhejiang Provincial Natural Science Foundation of China under Grant No. R1090134.

References

1. WAHL J. Articulated tool head: US, 6431802[P]. 2002-8-13.
2. NI Yanbing, ZHANG Biao, SUN Yupeng, et al. Accuracy analysis and design of A3 parallel spindle head[J]. *Chinese Journal of Mechanical Engineering*, 2016, 29(2): 239–249.
3. SICILIANO B. The Tricept robot: Inverse kinematics, manipulability analysis and closed-loop direct kinematics algorithm[J]. *Robotica*, 1999, 17(04): 437–445.
4. ZHAO Yanqin, JIN Yan, ZHANG Jun. Kinetostatic modeling and analysis of an Exechon parallel kinematic machine(PKM) module[J]. *Chinese Journal of Mechanical Engineering*, 2016, 29(1): 33–44.

5. LI Q, HERVÉ J M. Type synthesis of 3-DOF RPR-equivalent parallel mechanisms[J]. *IEEE Transactions on Robotics*, 2014, 30(6): 1333–1343.
6. LI Qinchuan, CHEN Qiaohong, YU Xufeng, et al. 3-DOF parallel mechanism with two perpendicular and non-intersecting axes of rotation: CN, 201110357878.7[P]. 2011-11-11. (in Chinese).
7. JIN Y, KONG X, HIGGINS C, et al. Kinematic design of a new parallel kinematic machine for aircraft wing assembly[C]//*Proceedings of the IEEE 10th International Conference on Industrial Informatics*, Beijing, China, July 25–27, 2012: 669–674.
8. LI Qinchuan, WU Weifeng, XIANG Jinan, et al. A hybrid robot for friction stir welding[J]. *Proceedings of the Institution of Mechanical Engineers, Part C: Journal of Mechanical Engineering Science*, 2015, 229(14): 2639–2650.
9. HUANG T, LI M, ZHAO X M, et al. Conceptual design and dimensional synthesis for a 3-DOF module of the TriVariant-a novel 5-DOF reconfigurable hybrid robot[J]. *IEEE Transactions on Robotics*, 2005, 21(3): 449–456.
10. LIU X, WANG J, PRITSCHOW G. A new family of spatial 3-DoF fully-parallel manipulators with high rotational capability[J]. *Mechanism and Machine Theory*, 2005, 40(4): 475–494.
11. XIE Fugui, LI Tiemin, LIU Xinjun. Type synthesis of 4-DOF parallel kinematic mechanisms based on Grassmann line geometry and atlas method[J]. *Chinese Journal of Mechanical Engineering*, 2013, 26(6): 1073–1081.
12. LI Y, STAICU S. Inverse dynamics of a 3-PRC parallel kinematic machine[J]. *Nonlinear Dynamics*, 2012, 67(2): 1031–1041.
13. XU Lingmin, LI Qinchuan, YE Wei. A 2R1T parallel mechanism with high rotational capability: CN, 201621160907.5[P]. 2016-10-25. (in Chinese).
14. HERVÉ J M. Analyse structurelle des mécanismes par groupe des déplacements[J]. *Mechanism and Machine Theory*, 1978, 13(4): 437–450.
15. LI Q, HUANG Z, HERVÉ J M. Type synthesis of 3R2T 5-DOF parallel mechanisms using the Lie group of displacements[J]. *IEEE Transactions on Robotics and Automation*, 2004, 20(2): 173–180.
16. LI Qinchuan, XU Lingmin, YE Wei. A 2R1T parallel mechanism with fixed actuators: CN, 201621253330.2[P]. 2016-11-22. (in Chinese).
17. LI Qinchuan, XIANG Jinan, CHAI Xinxue, et al. Singularity analysis of a 3-RPS parallel manipulator using geometric algebra[J]. *Chinese Journal of Mechanical Engineering*, 2015, 28(6): 1204–1212.
18. LI Shihua, LIU Yanmin, CUI Hongliu, et al. Synthesis of branched chains with actuation redundancy for eliminating interior singularities of 3T1R parallel mechanisms[J]. *Chinese Journal of Mechanical Engineering*, 2016, 29(2): 250–259.
19. MERLET J P. Redundant parallel manipulators[J]. *Laboratory Robotics and Automation*, 1996, 8(1): 17–24.
20. NOKLEBY S B, FISHER R, PODOHORODESKI R P, et al. Force capabilities of redundantly-actuated parallel manipulators[J]. *Mechanism and Machine Theory*, 2005, 40(5): 578–599.